Ion-beam effects on optical and rheological properties of polystyrene

L. Calcagno, G. Compagnini, and G. Foti
Dipartimento di Fisica, Corso Italia 57, 95129 Catania, Italy
(Received 18 June 1991; revised manuscript received 20 April 1992)

Ion-beam irradiation induces large changes in optical and rheological properties of polystyrene films. High-energy (100–300 keV) ion irradiations in the fluence range $10^{11}-5\times10^{14}$ ions/cm^2 produces optical defects in the original polymer chains (MW=9000 amu). A linear dependence on ion fluence has been detected up to a defect density of 2×10^{20} def/cm^3. Defect production rate depends on the energy loss of incoming ions and the chemical yield (bonds/100 eV) increases from 0.07 to 0.28 going from an energy loss of 10 eV/Å to 20 eV/Å, being the difference related to the spatial energy distribution inside the ion track. Rheological behavior, as solubility and molecular weight distribution, is modified after irradiation because the formation of cross-links between the main chains. The cross-link density exhibits a linear trend at low fluence ($\leq 10^{14}$ ions/cm^2) and a saturation at high fluence ($10^{14}-10^{15}$ ions/cm^2), when an average number of one cross-link per chain is produced. Correlation between optical and rheological data suggests that only optical measurements are correlated to the total bonds produced by ion irradiation in all the fluence range.

I. INTRODUCTION

Ion beams have became an integral part of several surface-processing and surface-layer modifications of solids.[1] Recently, there has been a growing interest in high-energy (keV-MeV) ion modifications of polymers[2,3] and other insulating materials.[4] In this regime the incident ion primarily undergoes electronic energy loss; since a typical ion such as 200 keV Ne deposits about 40 eV/Å in a typical carbonaceous material (density about 1.2 g/cm^3), an enormous amount of energy will be deposited inside the ion track.[5] Thus, by high-energy ions, one can study the nonlinear response of the material by producing intense local excitations without macroscopic thermal effects. The use of polymers as targets is a useful tool for understanding the radiation effects in organic materials, mainly because of the relative simplicity of the observed effects.[6]

In the last few years, the effects of ion beams on polymers have been investigated in different laboratories: Davenas *et al.*[7] and Fink *et al.*[8] have studied the changes in the optical and electrical properties of some polymers after high-energy (100–500 keV) irradiation. The conductivity change of polymers and organic materials has been largely investigated by Forrest *et al.*[9] and doping effects by Wnek, Dresselhaus, and Wasserman.[10]

Modifications of polymethylmethacrylate (PMMA) and polystyrene (PS) by very-high-energy (GeV) ions has been recently investigated and compared with the effects induced by KeV-MeV ions.[11] Technological application of ion-beam irradiations of polymer for a lithographic process has been reported by Gamo *et al.*[12]

We have performed a detailed study of ion-beam effects on polystyrene whose main advantage is related to its simple composition. Ion irradiation of polymers containing aromatic rings, which behave as an energy sink,[13] induces chain cross-links rather than scission, and then considerable modifications in the rheological properties (molecular weight distribution and solubility) will result.[14] Moreover, high-fluence irradiation of polystyrene induces a complete change of the original structure and the production of a new carbonaceous material, whose properties are similar to those of hydrogenated amorphous carbon.[15] The aim of this paper is to investigate the change in the optical and rheological properties of polystyrene thin films after low-fluence irradiation of different high-energy ions; moreover, the influence of the type of ion on this process will be investigated.

II. EXPERIMENTAL DETAILS

Polystyrene films, obtained by spinning a liquid solution of $CHCl_3$ on silicon and quartz substrate, were used in this work. Film thicknesses were 400, 250, and 10 nm, always smaller than the ion range to obtain a uniform energy deposition through the samples. Polystyrene of 9000 amu molecular weight was chosen with very low polydispersivity (1.06) to get a very narrow molecular weight distribution (MWD).

Films were then irradiated at room temperature with different ions and energies in order to change the energy loss (S) in a wide range, from 6 to 75 eV/Å. The ion-current density was always very low (50 nA/cm^2) to avoid any sample heating, and the total fluence ranges from 10^{11} to 5×10^{14} ions/cm^2.

UV-visible (200–800 nm) transmittance measurements were performed with double-beam spectrometry on samples deposited on quartz substrates. The molecular weight distributions of the PS films were determined by the Gel Permeation Cromatography (GPC) technique in the range 10^2-10^6 amu. The CPG system is equipped with a uv detector working at 260 nm of wavelength.[6]

III. RESULTS AND ANALYSIS

A. Optical measurements

Figure 1(a) reports the absorption spectra (A), in the 200–350-nm wavelength range, of ion-irradiated PS at different ion fluences of 300 keV H^+ together with the absorption spectrum of pristine sample (A_0). Unbombarded PS exhibits two bands in this wavelength range: one intense band at 220 nm and a weak absorption band at 260 nm. Both absorptions are associated to the π-electron system of aromatic rings: The intense band (220 nm) is ascribed to transitions to dipolar excited states, while the weak 260-nm band is related to forbidden transitions to homopolar excited states.[16]

Ion-beam irradiation induces large modifications of the 260-nm band [see Fig. 1(a)], where the vibrational structure, characteristic of pristine PS, is lost after ion irradiation and the optical spectra became smooth by increasing the ion fluence. Moreover, a large increase of the 260-nm-band intensity is detected after irradiation; instead, variations of the 220-nm band are not observed, at least for the film thickness used (250 nm). The ratio of the absorption coefficient of 220 nm with respect to the 260-nm band being a factor of 20, very thin films (~ 10 nm) have been used in order to detect any increase of the intense band after ion irradiation. The 220-nm band does not change in the irradiated polymer below 5×10^{14} ions/cm^2 for 300-keV protons; this result suggests that only a modification of the intense 260-nm band takes place after irradiation, and it is correlated to some new defect production and/or chemical modifications induced by the ion beam.

In order to eliminate the contribution of pristine absorption, we obtained the difference of absorption spectra ($A - A_0$) in the 240–350-nm wavelength range for the irradiated and pristine PS samples; the results are shown in Fig. 1(b) (as squares) for three different proton fluences. A possible approach to the analysis of the data is to assume an electron oscillator (Lorentz model) for the optical defect absorption, where each electron will be considered as a harmonic oscillator, with an oscillating frequency, a damping factor, and an amplitude determined from position, width, and height of the absorption spectra, respectively. In this model the absorption coefficient holds as

$$\alpha=\frac{8\pi^2e^2}{n\lambda\mu^*}N\frac{\gamma\omega}{(\omega_0^2-\omega^2)+\gamma^2\omega^2}\ , \tag{1}$$

where N is the electron density (or defect density), γ is the damping frequency, ω_0 is the oscillator frequency, m^* is the effective electron mass, n is the refractive index, λ is the wavelength, and e is the electron charge.

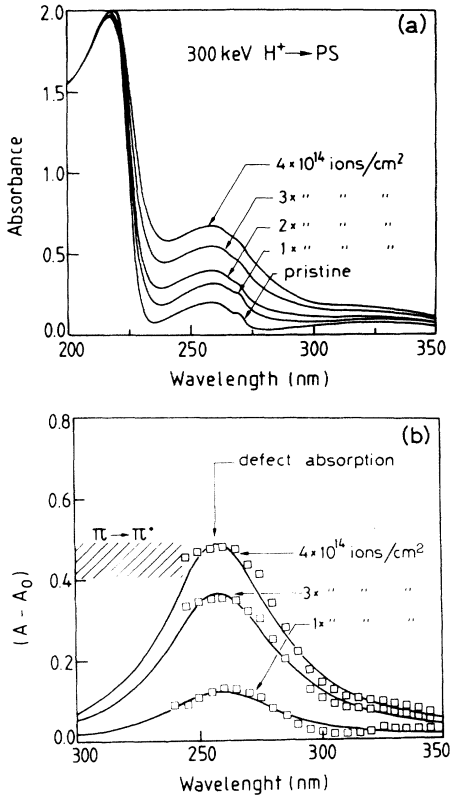

FIG. 1. (a) Optical-absorption spectra in the wavelength range 200–350 nm for PS samples irradiated at different fluences of 300-keV H^+ ions and for a pristine sample. (b) Absorbance difference of irradiated sample for different proton fluences and pristine PS.

From the experimental data of Fig. 1(b), we are able to get the position of maximum absorption ($\hbar\omega_0=4.8$ eV) and the damping energy ($2\hbar\gamma=1.1$ eV), which do not change with ion fluence and energy or ion mass, as given in Table I.

By fitting the absorption data reported in Fig. 1(a) for λ greater than 300 nm, we can obtain the refractive index (n) of irradiated PS. This value is almost constant after proton irradiation, going from 1.55 to 1.6 in the investigated ion-fluence range. Similar results have been obtained for He^+ and heavy-ion irradiations, where the refractive index shows variations within 3% with ion mass.

The effective electron mass (m^*) can be assumed as

TABLE I. Values of energy ($\hbar\omega_0$) and damping energy ($2\hbar\gamma$) for optical defects, energy loss (S), and chemical yield for cross-links (G_{CL}) and optical defects (G_{opt}) for different ions bombarding PS.

Ion energy	$\hbar\omega$ (eV)	$2\hbar\gamma$ (eV)	S (eV/Å)	G_{CL}	G_{opt}
300 keV H	4.8	1.1	6.5	0.07	0.07
100 keV He	4.8	1.07	16	0.26	0.27
200 keV Ne	4.8	1.1	40	0.28	0.27
400 keV Ar	4.8	1.05	75	0.29	0.28

equal to the free electron mass, because the features associated with the defects in the absorption spectra are quite sharp and these defects can be considered still as molecular bonds.

A more impressive way to interpret the defect behavior in PS is to refer to the defect absorption cross section, given by

$$\sigma=\alpha(N)^{-1}, \tag{2}$$

which include all the mentioned parameters, and it is constant for all the investigated ions and fluences and is equal to 1.1×10^{-16} cm^2 with a variation within few percent.

The theoretical value $(A-A_0)=\sigma Nx$ (with x the sample thickness) can be evaluated from relation (2) for different values of N to fit the experimental spectra. The results are reported in Fig. 1(b) as solid lines assuming for N the values 5×10^{19}, 2×10^{20}, and 2.7×10^{20} defects/cm^3, respectively. The good agreement between the experimental and calculated spectra in the entire wavelength range is noteworthy.

Figure 2 reports the obtained defect density (or electron density) versus ion fluence for 300-keV protons irradiation and for two sample thicknesses (250 and 400 nm). The defect density increases linearly with fluence, and no dependence on initial thickness and molecular weight of polymers has been detected. Ion-beam irradiation produces defects at a constant rate, which, for 300-keV H^+ irradiation at room temperature, is 12 defects/ion. Similar results have been obtained for PS irradiated with different ions; the fluence dependence is always linear for all ions, but the ion-fluence range shifts toward lower values for helium and heavy ions. The defect production rate increases to 100 defects/ion for helium ions.

A convenient parameter[17] to interpret ion-beam effects on polymers is the deposited energy density (eV/cm^3), $\epsilon=10^8\phi S$, where ϕ is the ion fluence (ions/cm^2) and S is the energy loss (eV/Å), as given in Table I.

Figure 3 reports the defect density, as obtained from optical measurements, versus the ϵ parameter for proton and helium irradiation. Again, the defect density increases linearly with energy density in both cases, but the slope relative to the helium-ion curve is a factor of 4

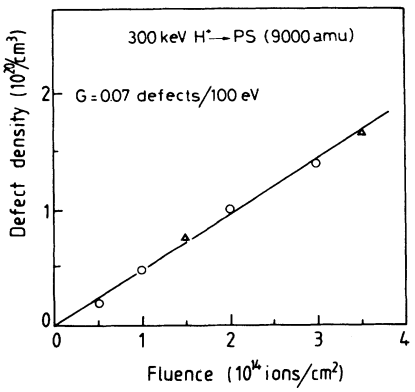

FIG. 2. Defect density vs ion fluence for 300 keV H^+ irradiating PS 400 nm (▲) and 250 nm (○) thick.

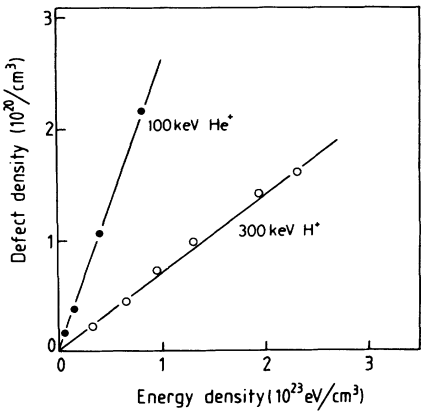

FIG. 3. Defect density vs energy density for protons and helium bombarding PS samples.

higher with respect to that of proton ions. Of course, the defect production rates will be different, and if we refer to the number of defects produced by 100 eV of ion-deposited energy, i.e., the so-called chemical yield G, we obtain 0.07 for protons and 0.28 for helium ions.

B. Rheological measurements

In the same ion-fluence range, besides optical properties, modification of rheological properties (MWD and solubility) has been detected in irradiated polystyrene. The MWD's of pristine 9000 amu PS and samples irradiated at different fluences of 300-keV H^+ ions are reported in Fig. 4, where all the experimental distributions have been normalized to the main peak. Because the starting PS has a very sharp distribution, even at very low fluences (1.5×10^{13} ions/cm^2), the MWD exhibits a second peak of molecular weight equal to 1.8×10^4 as a

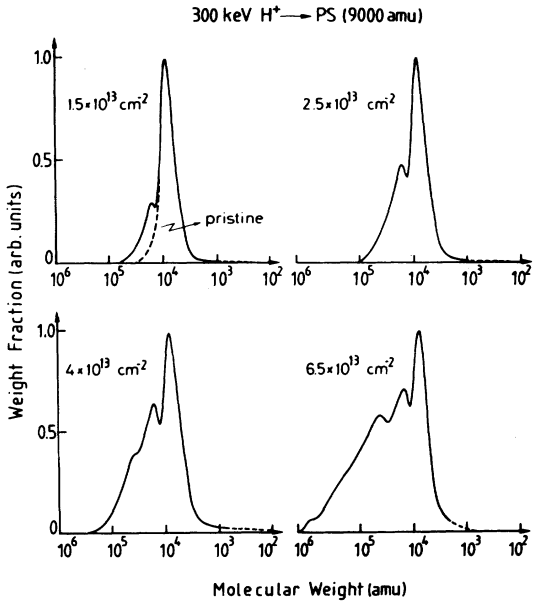

FIG. 4. Molecular weight distribution of samples irradiated at different fluences of 300 keV H^+ (pregel region).

result of formation of one cross-link between the original polymer chains. The new peak in the MWD is correlated to the formation of dimers in the PS.

At an ion fluence of 4×10^{13} ions/cm^2, chains with MW up to 10^5 are detected, because of the presence of trimers and n-mers; however, only the dimer peak is always well resolved. At high ion fluence (6.5×10^{13} ions/cm^2), overlap of each contribution gives a continuum distribution in the GPC signal.

The MWD's reported in Fig. 4 refer to a condition where the sample is fully soluble (pregel region), even the fraction at high molecular weight.

At very high ion fluence (10^{14} ions/cm^2), a fraction of the polymer becomes unsoluble (gel region), as shown in Fig. 5, where the MWD's are reported together with the soluble (s) and unsoluble (g) fractions (histograms in Fig. 5) for different ion-fluence irradiations. The soluble fraction of the polymer decreases with ion fluence and becomes zero when the whole polymer mass is transformed into a three-dimensional network. In the gel region, the MWD's show the presence of a small fraction of molecules related to scissions events (dashed line); however, it is always negligible in weight (few %) if it is compared with the total PS weight.

Similar results have been obtained for He^+, Ne^+, and Ar^+ irradiations, where the MWD's exhibit a similar behavior in shape as for H^+ irradiation but shifted toward lower ion fluences.

A very interesting way to analyze the results of the MWD and solubility is to consider the parameter X, which gives the number of cross-links per chain produced by ion irradiation in the original polymer chains. A statistical description of the MWD modification is already available when a given number of new bonds are introduced in the original distribution of a monodisperse polymer.[18,19]

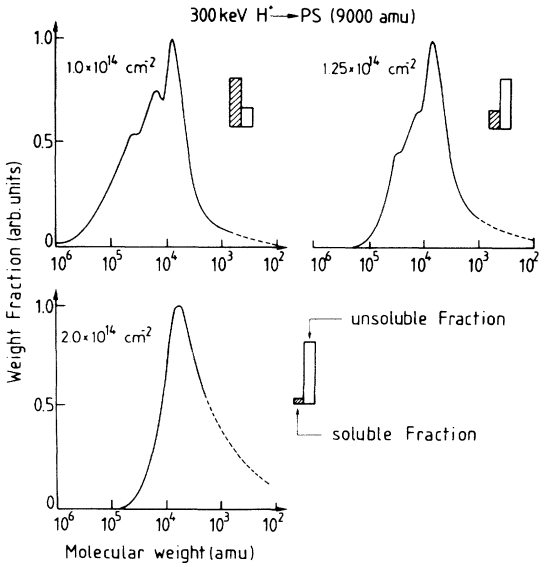

FIG. 5. Molecular weight distribution of PS irradiated at different fluences of 300 keV H^+ (gel region). The histograms of soluble and unsoluble fractions are also reported.

The basic assumptions of this model are the following: (1) New bonds between the chains are randomly distributed. (2) Each monomer has the same probability to form a new bond regardless its position in the chain, and (3) only interchain bonds (cross-links) are effective for the MWD and solubility change. All these hypothesis are compatible with our homogeneous polystyrene system and with ion-irradiation mechanisms, where the ionization-excitation events are randomly distributed in the polymer matrix.

From the proposed statistical model, it is possible to get the weight fraction of unperturbed MW (w_1) and of the unsoluble fraction (g) versus the number of cross-links per chains, as reported in Fig. 6(a). The w_1 parameter exhibits an exponential decrease in the entire range of X, while the unsoluble fraction is zero in the pregel region (i.e., below $X=0.5$) and it increases very fast for X above 0.5, reaching a value close to 1 for a number of cross-links per chains equal to 1.5.

From the experimental MWD and solubility measurements, we can measure the values of w_1 and the unsoluble fraction (g) in the gel region, as reported in Fig. 6(b), for 300-keV proton irradiation. By comparing the experimental data and expected values of w_1 and g, we are able to get a very interesting relation between the number of cross-links per chains (X) and the ion fluence (ϕ), as shown in Fig. 6(c).

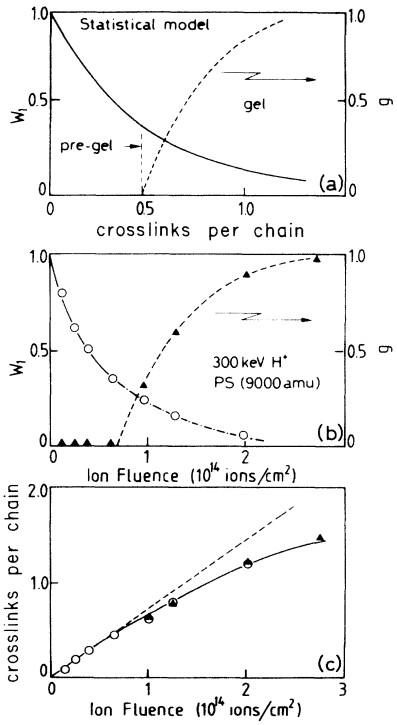

FIG. 6. (a) Weight fraction of initial MW (w_1, left ordinate scale) and unsoluble fraction (g, right ordinate scale) vs the number of cross-links per chains as obtained by a statistical model. (b) Weight fraction of initial MW (left ordinate scale) and unsoluble fraction (right ordinate scale) as a function of ion fluence as obtained from experimental results. (c) Cross-links per chains vs ion fluence for 300 keV H^+ irradiating PS samples.

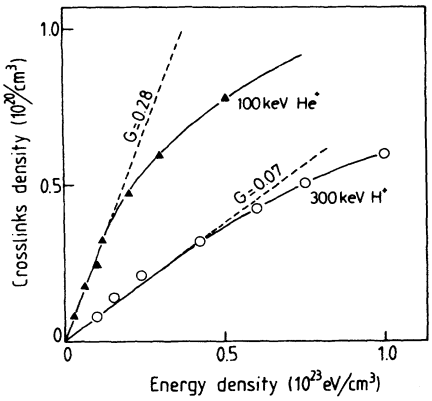

FIG. 7. Cross-link density vs the deposited energy density for H^+ and He^+ ions bombarding PS samples.

At low ion fluence, a linear relationship between X and ϕ is still valid as for the defect production, while by increasing the ion fluence a saturation behavior is observed.

From the X parameter, we can obtain the cross-link density (cross-link/cm^3), given by the product of the cross-links per chains and the cross-link density (chain/cm^3), and from ion fluence and energy loss we get the energy density (ϵ). In Fig. 7 both quantities are reported for H^+ and He^+ irradiation. Of course, the cross-link density increases linearly with energy density and saturates at high values, as observed for the ion-fluence behavior. The linear region extends up to 1.2×10^{22} eV/cm^3 for helium ions and up to 5×10^{22} eV/cm^3 for protons. In this region the slope is higher for helium ions, with respect to that for protons, and from that we obtain a chemical yield for cross-link production of 0.07 and 0.28 for protons and helium ions, respectively. These values are the same as that obtained from optical measurements for the chemical yield of defect production.

IV. DISCUSSION

The predominant effect of ionization radiations on polystyrene is the production of defects in the original polymer structure; these defects are quite stable and give a specific absorption peak around the 260-nm wavelength region, observed as in the solid film deposited on a transparent substrate as in a liquid solution (pregel region). The absorption cross section (σ) is almost constant with a few percent difference for all the investigated ions (protons, helium, etc). Defects can be considered as new bonds, and a possible mechanism is the weakness of the π electronic system of the phenil ring and the synthesis of alkene-type bonds.[20] The production rates of defects or new bonds produced by ion irradiation, as deduced from optical data, are nicely correlated with solubility and MWD measurements, at least when the energy deposited in the sample is quite low.

The cross-link production rate of protons is about a factor of 4 lower compared with the other ions, and it is 0.07 cross-links/100 eV, given as a chemical yield. The dependence of the chemical yield for defect and cross-link production, on the ion energy loss (S), is very similar for 300 keV H^+, 100 keV He^+, 200 keV Ne^+, and 400 keV Ar^+, supporting the basic idea that the involved mechanism at the microscopic level is the same.

However, the values of the chemical yields as reported in Table I depend on ion mass: This dependence must be related to the energy-transfer mechanism between the incoming ion and electrons in the target, and a detailed description of the ion track would be necessary. Ion energy deposition produces a nonhomogeneous spatial distribution of primary precursors (ionized species, excited species, radicals, etc., which can recombine or react within a volume much larger than that of the ion track, as a result of the contribution of the diffusion process of reactive species or to the propagation of radicals along the chain. The concentration and spatial distribution of these reactive species determine the value of G for defect production, which can be considered as new bonds in the polymer structure.

For light ions the tracks consist of a series of "spurs" whose average separation is a few thousand of Å, while for heavy ions this distance is strongly reduced (1–10 Å). In the last case, reactions between the spurs of different tracks or the same track can occur; these reactions give a high yield of elementary events and can explain the observed difference in the defect production rate between light ions as protons and heavy ions.

The cross-link yield measured with very-high-energy ions in the MeV-GeV energy region and reported in the literature[12] shows very similar behavior to proton irradiation. This unexpected result points out that a better description of the ion track is necessary and, maybe, together with the energy loss value, the detailed spatial distribution of excited electrons is important to understand the effects induced in the polymer target by ion irradiation, as the cross-link production rate for high values of energy loss.

The cross-link density, obtained from rheological measurements, and defect density, from optical measurements, exhibit a very interesting correlation if plotted together for the same ion energy density. In Fig. 8 are reported the experimental results and it is clear that all data collapse in a single curve. This result is very important because it has been tested in a wide range of ion fluence or energy density and for different incoming ions. It must be stressed that the defect production rate for protons is low compared with that of helium or heavy-ion

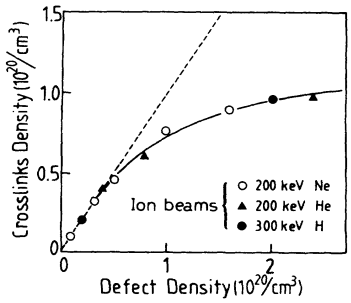

FIG. 8. Cross-link density vs defect density for different ions bombarding PS.

irradiations, as is cross-link production, but the cross-link density versus defect density gives a unique curve. Because all the experimental data are fitted by a single curve, it means that the basic mechanism for defect and cross-link production is the same or, maybe, the same new bonds introduced by ion irradiation are responsible for cross-links and for the strong optical absorption.

The saturation behavior in the cross-link density, at high defect density ($10^{20}/cm^3$), is related to rheological measurements which are sensitive to the molecular weight of the new chains produced by ion irradiation regardless of the total number of bonds. This result suggests that rheological measurements allow one to measure the bonds needed to produce an n-mer of the original chain and/or a given gel fraction, while optical measurements give the absolute number of new bonds induced by ion irradiation regardless of the properties (molecular weight and solubility) of new chains.

It is important to stress that the picture given in the present work to interpret the ion-beam effects on optical and rheological properties of PS, in terms of new stable bonds, does not require a detailed description of the ion track behavior. Only the assumptions for the defect absorption mechanism and statistical distribution of bonds occur.

V. CONCLUSIONS

Changes in the optical and rheological properties of polystyrene induced by ion irradiation are due to the formation of new bonds. Both types of measurement give the same trend for all the investigated ions, but only optical measurements are sensitive to the total amount of bonds in the entire fluence range.

The production rate for defects and cross-links depends upon the specific ion: It is a factor of 4 higher for heavy ions with respect to protons, regardless of the total deposited energy after irradiation. This result suggests that the energy distribution inside the single-ion track is the controlling factor for the chemical yield. However, the correlation between the optical defect and cross-link densities points out that the basic mechanisms to understand the effects induced by ion irradiation are the same.

ACKNOWLEDGMENTS

The authors thank Professor G. Mondio and Professor O. Puglisi for the helpful discussions and interpretation of experimental data. This work was supported by Progetto Finalizzato "Materiali e dispositivi per l' elettronica dello stato solido" of Consiglio Nazionale delle Ricerche (Roma).

[1]J. S. Williams and J. M. Poate, *Ion Implantation and Beam Processing* (Academic, New York, 1984).

[2]J. Davenas, P. Thevenard, G. Boiteaux, M. Fallavier, and X. L. Lu, Nucl. Instrum. Methods B **46**, 317 (1990).

[3]T. Venkatesan, L. Calcagno, B. S. Elman, and G. Foti, in *Ion Beam Modification of Insulators,* edited by P. Mazzoldi and G. W. Arnold (Elsevier, Amsterdam, 1987), Vol. 2, p. 301.

[4]P. Mazzoldi and G. W. Arnold, in *Ion Beam Modifications of Insulators,* (Ref. 3), Vol. 2, p. 195.

[5]*Heavy Ions Stopping and Ranges,* edited by J. F. Ziegler and H. H. Anderson (Pergamon, New York, 1977).

[6]O. Puglisi, A. Liccialdello, L. Calcagno, and G. Foti, Nucl. Instrum. Methods B **19/20**, 865 (1987).

[7]J. Davenas, X. L. Xu, G. Boiteaux, and D. Sage, Nucl. Instrum. Methods B **39**, 759 (1989).

[8]D. Fink, M. Muller, L. T. Chadderton, P. H. Cannington, R. G. Elliman, and D. C. McDonald, Nucl. Instrum. Methods B **32**, 215 (1988).

[9]S. R. Forrest, M. L. Kaplan, P. H. Schmidt, T. Venkatesan, and A. J. Lovinger, Appl. Phys. Lett. **41**, 706 (1982).

[10]G. E. Wnek, M. S. Dresselhaus, and B. Wasserman, in *Ion Implantation and Ion Beam Processing of Materials,* Proceedings of MRS Symposium, edited by G. K. Hubler, O. W. Holland, C. R. Clayton, and C. W. White (North-Holland, Amsterdam, 1983), Vol. 27, p. 413.

[11]W. Schnabel and S. Klaumunzer, Radiat. Phys. Chem. **33**, 323 (1989).

[12]K. Gamo, K. Yamashita, F. Emoto, and S. Namba, J. Vac. Sci. Technol. B **3**, 117 (1985).

[13]A. Chapiro, Nucl. Instrum. Methods B **32**, 111 (1988).

[14]O. Puglisi, A. Licciardello, L. Calcagno, and G. Foti, J. Mater. Res. **3**, 1247 (1988).

[15]G. Compagnini, G. Foti, R. Reitano, and G. Mondio, Appl. Phys. Lett. **57**, 1 (1990).

[16]*Uv and Visible Spectrometry, Chemical Applications,* edited by C. N. R. Rao (Butterworths, London, 1975).

[17]L. Calcagno, G. Foti, A. Licciardello, and O. Puglisi, Appl. Phys. Lett. **51**, 907 (1987).

[18]P. J. Flory, J. Chem. Phys. **46**, 132 (1942).

[19]P. J. Flory, J. Am. Chem. Soc. **63**, 3091 (1941).

[20]O. Puglisi, A. Licciardello, S. Pignataro, L. Calcagno, and G. Foti, Radiat. Eff. **98**, 161 (1986).